A Real-Time Bicycle Record System of Ground Conditions based on Internet of Things

Yu-Xiang Zhao, Yu-Sheng Su, and Yao-Chung Chang, Member, IEEE

Abstract—In recent years, bicycles have quickly become one of the major urban sports. At the same time, with the rise of Internet of Things (IoT), embedded system combine IoT devices are widely used and making computing truly ubiquitous. Although bicycles have various functions, they fail to provide cyclists with sufficient exercise-related information and post-exercise analysis. Therefore, this study introduced a bicycle record system of ground conditions based on IoT which is combining smartphone and embedded system. The event data recorder comprised two parts, a "smartphone-based event data recorder" and "bicycle-based real-time information feedback system." Using the event data recorder, this study integrated and provided various types of real-time information for cyclists while they cycled to help them achieve their desired exercise results. After cycling, the cyclists could view cycling-related information through software analysis. This information included cycling routes taken, total cycling distance, and total calories burned. The event data recorder also saved information related to cycling routes such as acceleration, deceleration, directional changes, and slope changes. By analyzing the recorded information, cyclists not only gained further insight into their exercise results but were also able to share cycling-related information through the Internet, which would benefit cyclists who had not cycled along this route before. By developing the bicycle record system, this study aimed to provide cyclists with real-time, accurate, and complete information, enabling them to enjoy a consummate cycling environment.

Index Terms—Bicycles, Internet of Things, Cellular phones, Embedded software, Event detector

I. INTRODUCTION

In recent years, the rapid development of cycling in Taiwan has increased the public visibility of cyclists. Because cycling is healthy, environmentally friendly, and internationally popular, it has emerged as a city sport. Modern bicycles have various styles and functions, and ease of use has become crucial for bicycle design [1]. Bicycles can primarily be divided into the following categories: road bicycles, mountain bicycles, folding bicycles, and electric bicycles. Although bicycles have a myriad of functions, they fail to provide cyclists with sufficient exercise-related information while they cycle. For example, contrary to professional cyclists, who train with coaches, average cyclists cannot ascertain whether they have achieved their desired exercise results while cycling. This has contributed to a loss of motivation and interest in cycling. At the same time, the concept of the Internet of Things (IoT) is putting forward a vision where the Internet is extending into the real world, connecting physical items to the virtual world and making computing truly ubiquitous. Smart objects with embedded information and communication technology are considered an essential building block of this vision. IoT idea, in general, is expected to be opening up huge opportunities for individuals as well as the entire economy [2-3]. Building upon the unique availability of electrical power on e-bikes, numerous initiatives have started exploring the implementation of sensing devices also on e-bikes, e.g., [4]. moreover, we have found evidence that the data collected by such devices may in the form of social normative feedback ultimately be useful in influencing people's travel mode choice [5]. Thus, identifying an efficient method to obtain cycling-related information is key to designing new-generation bicycles. The use of embedded systems with sensors has, therefore, become increasingly common. Currently, cyclists' experiences are typically converted into numerical data, which are collected for dietary, health, and fitness measurements [6]. The sensor systems used for bicycles typically display basic data such as wheel speed; total riding distance and calories burned are also calculated through simple deduction. As technology advances, these systems also increase in function and decrease in volume. Embedded systems in bicycles can be employed in a variety of fields [7-10] such as parking lot management [7], position trajectory management [8], and particularly in bicycle-based rehabilitation [9] and cycling posture management [10]. Moreover, because of their growing popularity, smartphones have also increasingly used sensors. These sensors include inertial sensors, G-sensors, M-sensors, gyroscopes, short range sensors, and ambient light sensors. Smartphones with these sensors are therefore used for various purposes [11-16] such as tracking user coordinates through GPS [11], recording the number of steps walked, caring for
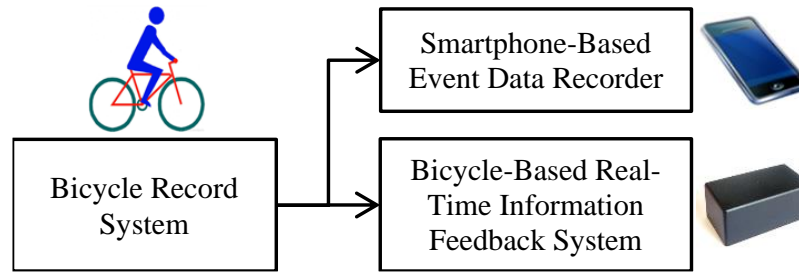
Fig. 1. System architecture.

elder people, and preventing falls [12-14]; smartphones are even more widely used in fitness games [15-16]. Therefore, when designing embedded systems for bicycles, designers may use smartphones as replacements for sensors to acquire information. This reduces the volume and capacity of embedded systems as well as power consumption. Therefore, this study presented a bicycle record system of ground conditions based on IoT. This recorder was constructed by combining a smartphone with an embedded system. The event data recorder, which comprised a "smartphone-based event data recorder" and "bicycle-based real-time information feedback system," displayed and recorded cyclists' exercise-related information while they cycled. Regarding hardware planning and design, this study assumed that all cyclists carried smartphones at all times because of the popularity and convenience of these devices. This substantially reduced the development cost of the event data recorder. In this study, the sensors used by smartphones were categorized as "smartphone-based event data recorders" and divided into five modules according to their function. The five modules were the accelerometer, gyroscope, electric compass, GPS route, and system integration modules. To obtain cyclists' real-time information when cycling, a bicycle-based real-time information feedback system was built and divided into three modules based on function. The three modules were the reed switch, real-time information display, and Bluetooth transmission modules. Through the event data recorder, this

study aimed to integrate various types of real-time information and provide them to cyclists when they cycled to help them achieve their desired exercise results. In addition, the technology developed in this study enables cyclists to view cycling-related information through software analysis after they completed cycling. This information includes the cycling routes taken, total cycling distance, average speed, and total calories burned. The event data recorder also saves cycling route-related information such as slope changes and road conditions. Such information is useful for cyclists who have not cycled along the route before. By analyzing the recorded information, cyclists not only gain insight into their exercise results but can also share cycling-related information through the Internet. In developing the bicycle record system, this study aimed to provide cyclists with accurate real-time information, enabling them to enjoy a consummate cycling environment.

II. SYSTEM DESIGN

This study introduced a bicycle record system that combined a smartphone with an embedded system to record and provide cyclists with exercise-related information when they cycled. The event data recorder comprised two parts, which were a "smartphone-based event data recorder" and "bicycle-based real-time information feedback system," as shown in Figure 1. Detailed information on the two parts is provided in the following sections.
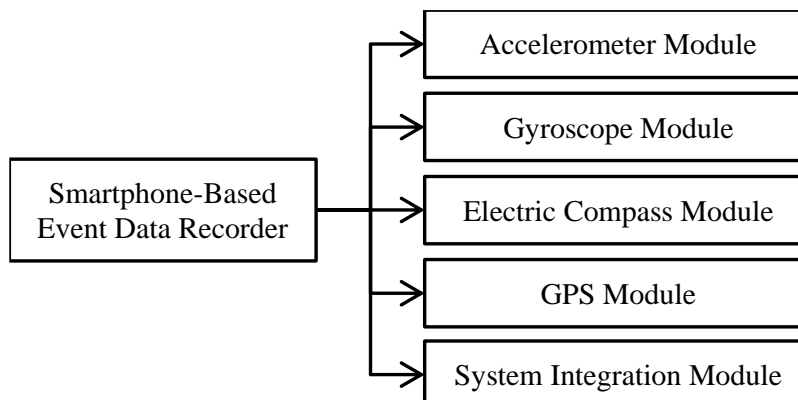
Fig. 2. Modules of the smartphone-based event data recorder.

A. Smartphone-Based Event Data Recorder

The smartphone-based event data recorder consisted of five modules, which were the accelerometer, gyroscope, electric compass, GPS route, and system integration modules, as shown in Figure 2. Detailed descriptions of the modules are presented in the following sections.

Accelerometer Module

For the accelerometer module, this study used the three-dimensional (3D) accelerometers of smartphones to examine cyclists' acceleration direction. Figure 3 shows a diagram of the acceleration direction. Acceleration data can be used to analyze cycling habits and road conditions as well as prevent theft. Accelerometer functioning is based on the use of the heat conduction observed in heat convection. In other words, when an object accelerates in a direction, it creates disturbances in heat conduction, creating differences in the temperature of thermoelectric voltages measured from four directions; the output voltages also differ. The differences in electric potential can subsequently be used to determine the directions of acceleration because the differences in electric potential and direction of acceleration are directly proportional to each other.
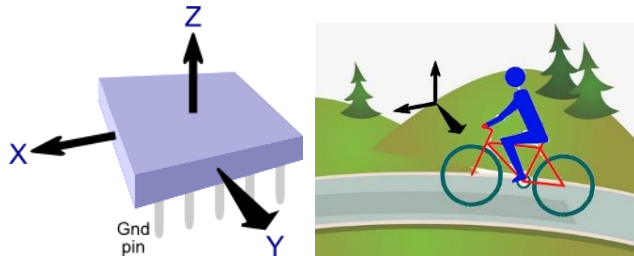

Fig. 3. Detect cyclist's acceleration direction.

Gyroscope Module

The 3D gyroscopes built in smartphones were used to determine cyclists' angles of rotation. Figure 4 illustrates the angles of rotation. This data can be used to determine whether cyclists are balanced, fatigued, or have poor cycling habits as well as whether their bicycles have overturned. Electronic gyroscopes, also called microelectromechanical gyroscopes,
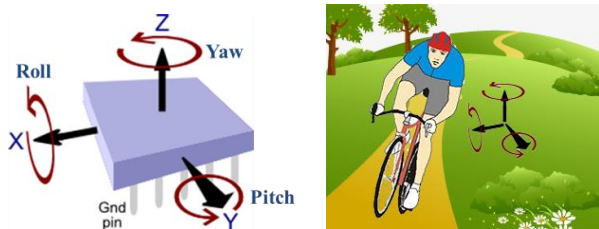
are semiconductor chips. These chips contain miniature magnetic material and detect the direction of movement during rotation.

Electric Compass Module

The 3D electric compasses of smartphones were used to determine cycling direction. Figure 5(a) provides a diagram of the cycling direction as shown on a compass. This information can be used to determine whether cyclists are cycling along the correct routes to travel to their destinations. Information about local wind direction can also be obtained through the Internet to determine whether cyclists are cycling downwind or upwind. Electric compasses, similar to traditional compasses, distinguish the North and South Poles by sensing the Earth's magnetic fields. Electric and traditional compasses are distinct because electric compasses use magnetoresistive sensors rather than magnetic needles. Additionally, electric compasses apply the principle of Hall effect to sense direction, using the direction of electron deviation in electric currents to calculate changes in voltage from which the directions of north and south can be identified.

GPS Module

For the GPS module, the GPS function of smartphones was used to determine cyclist coordinates. Figure 5(b) shows a diagram of GPS coordinates. GPS data can be used to record cyclists' coordinates when they are cycling. Cyclists may also share route maps generated from recorded data with other cyclists through the Internet. GPS relies on satellite triangulation by which distance is calculated by measuring the transmission time of radio signals; the calculated distance is subsequently used to determine the location of a satellite in space. The GPS method is an observation method that involves high orbit and precise positioning.
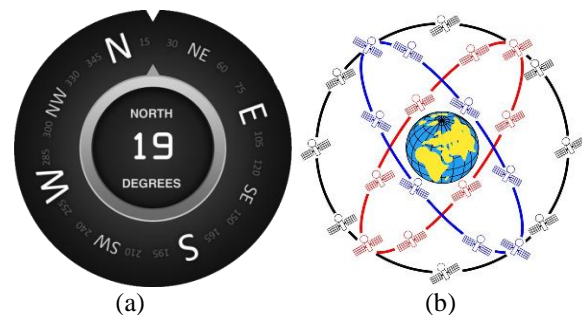

(a) (b)

Fig. 5. Module function diagram: (a) directions on a compass; (b) GPS coordinates.

Fig. 4. Detect cyclist's rotation angle.

System Integration Module

In this study, the system integration module read and organized the information provided by the aforementioned modules. The information, which was displayed in real-time on smartphone screens, was also stored in smartphones' memories. In addition, the system integration module used the built-in Bluetooth function of smartphones to connect to the Bluetooth transmission module of the bicycle-based real-time information feedback system to collect information. This information can be used to calculate and produce statistical results regarding cyclists' real-time speed, average speed, total distance traveled, and calories burned; these data are simultaneously displayed on and stored in smartphones. Through the system integration module, all software and hardware information can be integrated to produce data with optimal accuracy and stability and develop a bicycle record system that provides accurate real-time information. Regarding the design of the smartphone screen display, this study divided the system integration

Fig. 6. System integration module interface.

module interface into six parts, as shown in Figure 6. Descriptions of each of these items are as follows:

- (i) Positioning and tagging of the routes taken,
- (ii) State of connection between the smartphone and Bluetooth module,
- (iii) Cycling direction indicated by the electric compass module, D. Real-time bicycle speed information relayed by the bicycle-based real-time information feedback system,
- (iv) Information regarding total distance traveled relayed by the feedback system,
- (v) Weight of the cyclists, which is used to calculate

calories burned, and
- (vi) Total time engaged in cycling.

B. Bicycle-Based Real-Time Information Feedback System

The bicycle-based real-time information feedback system contained four modules: the control and computing, reed switch, real-time information display, and Bluetooth transmission modules. The system architecture is shown in Figure 7. Detailed descriptions of the modules are provided in the following sections.
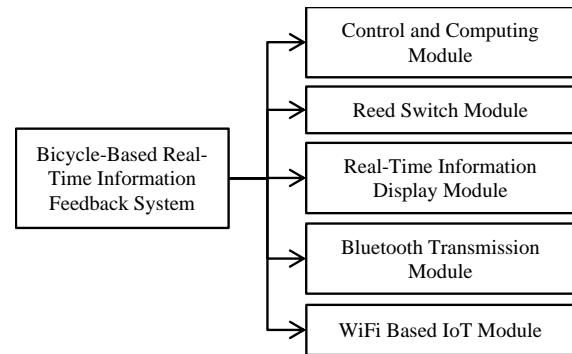

Fig. 7. Architecture of the bicycle-based real-time information feedback system.

Fig. 8. LinkIt 7697.

Fig. 9. Actual hardware image.

Control and Computing Module

LinkIt 7697 (as shown in Figure 8) is one of MediaTek's products which combines WiFi module and Bluetooth module. It was used as the basis for designing the bicycle-based real-time information feedback system in this study. An image of the hardware is shown in Figure 9. The system first reads

information provided by the reed switch module by using the Arduino while displaying related cycling information on the real-time information display module. Next, the system sent real-time cycling information back *to* smartphones through the Bluetooth transmission module.

Reed Switch Module

A reed switch was used to measure the number of wheel rotations and time required for wheels to complete one rotation. Reed switches function using reed tubes, which serve as the primary parts of devices that convert mechanical movement into electrical signals. When magnets approach the magnetic switches of devices, they cause the reed switches inside the magnetic switches to sense changes in the magnetic field. The reed switch contact point subsequently closes, thus completing the electric circuits, as shown in Figure 10.

Fig. 11. Image of reed switch installation.

Fig. 12. Diagram of a positive-edge trigger.

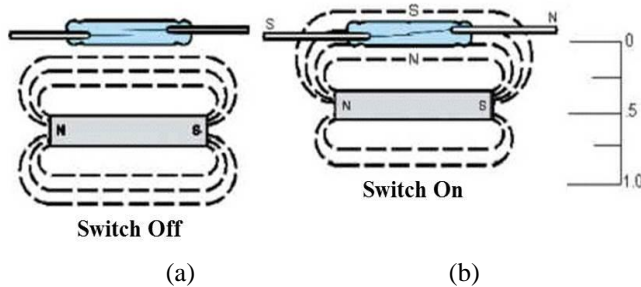

(a)   (b)

Fig. 10. Schematic diagram of the reed switch principle: (a) Switch Off; (b) Switch On.

In this study, reed switches were installed on bicycle wheels. The module was contacted once each time that a wheel completed one rotation, as shown in Figure 11. To prevent the module from being triggered more than once upon contact, the reed used the positive-edge trigger method as its method of judgment, as shown in Figure 12. When no contact is made (thus no trigger) for more than 15 seconds, the bicycle was determined to be at rest. According to the time interval between each trigger and number of times that the module was triggered, the real-time speed and mileage were determined. The formulas for calculating the two variables are shown as follows:

$$speed = \frac{length/1000}{time/(1000 \times 60 \times 60)}$$
$$= 3600 \times \frac{length}{time} \qquad (1)$$

$$distance = \frac{count \times length}{1000} \qquad (2)$$

where *speed* is the real-time speed (*km/h*) of the bicycle, *length* is the wheel circumference (*m*), *time* is the time interval between each wheel rotation (*ms*), *distance* is the mileage (*km*), and *count* is the number of wheel rotations.
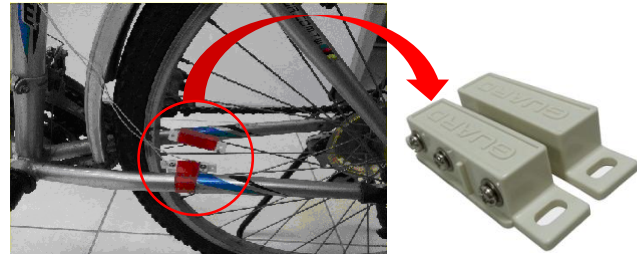
Real-Time Information Display Module

Information (e.g., speed and accumulated mileage) derived from the reed switch was displayed using the real-time information display module, as shown in Figure 13. This information was sent back to the smartphone-based event data recorder (i.e., the smartphone on the bicycle) through the Bluetooth transmission module. Accurate real-time exercise-related information was then calculated by the smartphone by using the calculation programs, and the information was displayed for cyclists. Furthermore, the information was recorded and saved by the smartphone, enabling cyclists to share their cycling information online.

Fig. 13. Real-time information display module interface.

Bluetooth Transmission Module

This module establishes a connection with the Bluetooth device built in the smartphone. The real-time information calculated by the reed switch module was then transmitted to the smartphone-based event data recorder, as shown in Figure 14.

Fig. 14. Bluetooth transmission.

WiFi-based IoT Module

This module uses WiFi, which is connecting to the 4G of the smartphone, to transmit the real-time bicycle information to cloud storage. The real-time bicycle information includes the speed calculated by the reed switch module, the acceleration direction calculated by the accelerometer module, rotation angle calculated by the gyroscope module, the compass direction calculated by the electric compass module, and GPS coordination calculated by the GPS Module. All the real-time bicycle information is transmitted to the cloud storage, as shown in Figure 15.

Fig. 15. Transmit information to the cloud storage.

III. PARAMETER ESTIMATION

The data recorder in this paper presents an orientation tracking algorithm based on the output data of a 3D accelerometer and a 3D gyroscope. Orientation estimation is executed with an unscented Kalman filter (UKF) whose parameters are varied in order to reduce the influence of motion. The UKF is an extension of the traditional Kalman filter for the estimation of nonlinear systems that attempt to remove some of the shortcomings of the extended Kalman filter (EKF) in the estimation of nonlinear systems. For parameter estimation, the EKF can be used, because the computation time of the UKF is greater than the computation time of the EKF. However, because there are no limitations with regard to computation time and it has been shown that the UKF outperforms the EKF in numerous examples, the UKF was chosen for parameter estimation. More detailed discussion of the UKF can be found in [17-19]. The UKF uses deterministic sampling to approximate the state distribution. The unscented

transformation uses a set of sample or sigma points that are determined from the a priori mean and covariance of the state. The sigma points are propagated through the nonlinear system. The posterior mean and covariance are then calculated from the propagated sigma points. Parameter estimation equations for the UKF are similar to the state estimation.

Kalman Filter has been the subject of extensive application and research, especially in the autonomous navigation and guided navigation areas. The Kalman Filter performs well in practice and attractive in theoretical because it can minimize the variance of the estimation error [20]. The small computational requirement, recursively properties, and status as optimal estimator are the great success of the Kalman Filter [21]. In this study, Kalman Filter is designed to reduce the noise on the sensor.

A. Input Vector

The input vector x of the Kalman filter must represent the 3D orientation of the sensor node. Therefore, it consists of three dimensions data:

$$x = [v_x \quad v_y \quad v_z]^T \tag{3}$$

B. Process and Measurement Model

The process model predicts the evolution of the state vector:

$$x_{k+1} = x_k + \gamma(x_k - x_{k-1}) + w_k \tag{4}$$
$$Q = q \cdot I_{3\times3} \tag{5}$$

where x_k is the processed state in time k and w represents the process noise with covariance matrix Q. The measurement model relates the measured value z to the value of the state vector x.

$$z = H(x) = [z_{acc} \quad z_{gyr}]^T = R \cdot x + v \tag{6}$$
$$R = \begin{bmatrix} r_{acc} \cdot I_{3\times3} & 0_{3\times3} \\ 0_{3\times3} & r_{gyr} \cdot I_{3\times3} \end{bmatrix} \tag{7}$$

where v represents the sensor noise with covariance matrix R. The output noise is assumed to be uncorrelated between the two sensors and between the different axes.

C. Prediction

The first step in the Kalman filter is the prediction, which is based upon (4). Since this is actually a linear equation, no sigma points have to be calculated yet.

$$\hat{x}_k^- = \hat{x}_{k+1}^+ + \gamma(\hat{x}_{k-1}^+ - \hat{x}_{k-2}^+) \tag{8}$$
$$P_k^- = P_{k-1}^+ + Q \tag{9}$$

This article has been accepted for publication in a future issue of this journal, but has not been fully edited. Content may change prior to final publication. Citation information: DOI 10.1109/ACCESS.2017.2740419, IEEE Access

7

D. Compute Sigma Points

Before the correction can be executed, sigma points must be computed from the mean and square root decomposition of the covariance of the a priori estimate.

$$x_k = \left[\hat{x}_k^-, \quad \hat{x}_k^- + \eta\sqrt{P_k^-}, \quad \hat{x}_k^- - \eta\sqrt{P_k^-} \right] \tag{10}$$

where $\eta = \sqrt{n + \lambda}$ is the state dimension, and λ determines the spread of the sigma points.

E. Measurement Prediction

From the computed Sigma Points, a prediction of the measurement can be made based on (6).

$$Z_k = H(X_k) \tag{11}$$

$$z_k^- = \sum_{i=0}^{2n} W_i^{(m)} Z_{i,k} \tag{12}$$

$$P_{z_k} = \sum_{i=0}^{2n} W_i^{(c)} \left(Z_{i,k} - z_k^- \right)^2 \tag{13}$$

$$P_{x_k z_k} = \sum_{i=0}^{2n} W_i^{(c)} \left(X_{i,k} - x_k^- \right) \left(Z_{i,k} - z_k^- \right)^T \tag{14}$$

where

$$W_i^{(m)} = W_i^{(c)} = \begin{cases} \lambda/n + \lambda & , i = 0 \\ \lambda/2(n + \lambda) & , i = 1 \dots 2n \end{cases} \tag{15}$$

F. Correction

This is where the actual measured data comes into play and the posteriori estimate is calculated.

$$K = P_{x_k z_k} \left(P_{x_k} + R \right)^{-1} \tag{16}$$

$$\hat{x}_k^+ = \hat{x}_k^- + K(z - z_k^-) \tag{17}$$

$$P_k^{\mp} = P_k^- - K\left(P_{z_k} + R \right) K^T \tag{18}$$

G. Postfilter

Finally, the posteriori estimate is low pass filtered.

$$\hat{x}_k^+ = \alpha\hat{x}_{k-1}^+ + (1 - \alpha)\hat{x}_k^+ \tag{19}$$

IV. EXPERIMENTAL RESULTS

A. System Parts

The bicycle record system introduced in this study contained a "smartphone-based event data recorder" and "bicycle-based real-time information feedback system." An image of the entire hardware model is shown in Figure 16.

Fig. 16. The bicycle record system.

B. Recording Platform

After cycling, information recorded in the smartphone-based event data recorder was saved in a recording platform through the Internet; this information was subsequently shared online. The cloud recording platform designed by ASP.NET was used to design the recording platform. The recorded information was converted to useful information and displayed on a webpage for user access. Cycling information was divided into five categories on the recording platform, namely route taken, cycling information, slope conditions, road conditions, and riding conditions, as shown in Figure 17. Detailed information on the five categories is provided as follows.
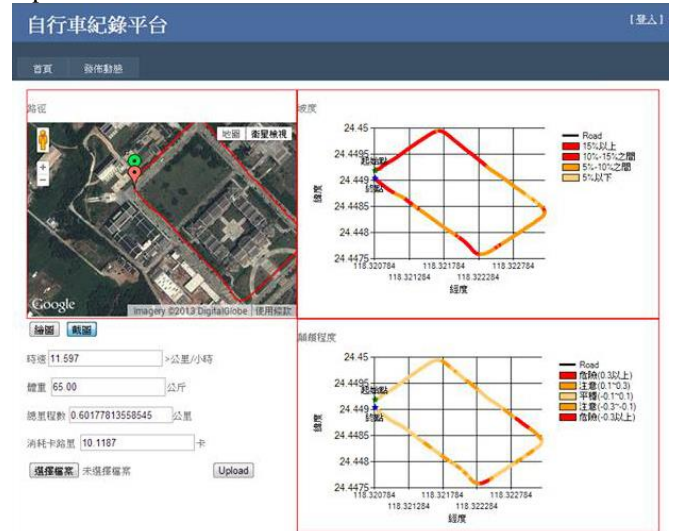

Fig. 17. Recording platform interface.

Route Taken

Regarding information on route taken, coordinates of the routes taken recorded by the GPS route module in the smartphone-based event data recorder were plotted on the Google Map accordingly, as shown in Figure 18.

Fig. 18. Routes taken.

Cycling Information

The cycling information comprised the following data:

(i) Average speed: The average of the speeds recorded at each recording point.
(ii) Weight of cyclist: Weight entered by the cyclist into the system integration module.
(iii) Total mileage: Total mileage calculated by the system.
(iv) Calories burned: Calculation was based on the information provided in Table 1.

Slope Conditions

Information on slope conditions showed the changes in slope for the cycling routes taken. Slope conditions were determined using the altitudes of the recording points obtained by the GPS route module to calculate the horizontal distances between the recording points. The following formula (20) was employed to calculate the slope changes, as shown in Figure 19.

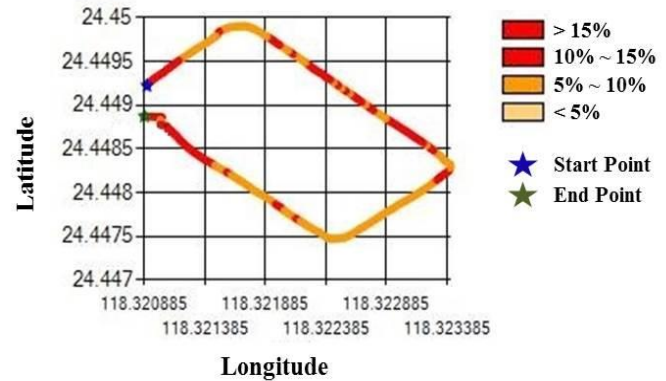$$Slope = \frac{Changes\ in\ altitude}{Changes\ in\ horizontal\ distance} \qquad (20)$$

Fig. 19. Slope changes.

Road Conditions

Road conditions referred to the bumpiness of the cycling routes taken. Data recorded by the accelerometer module were calculated and converted to simple information, as shown in Figure 20.
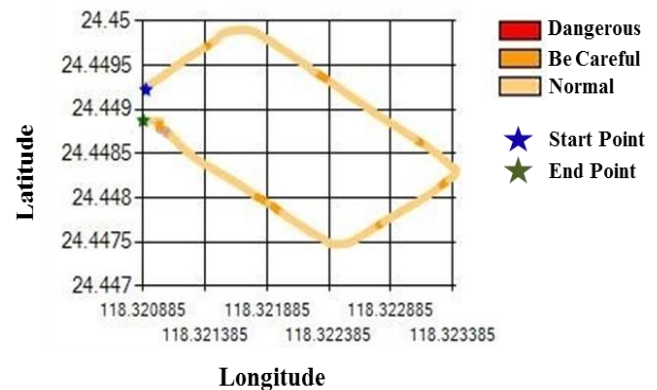

Fig. 20. Road conditions.

TABLE I
REFERENCE TABLE FOR CALORIES BURNED

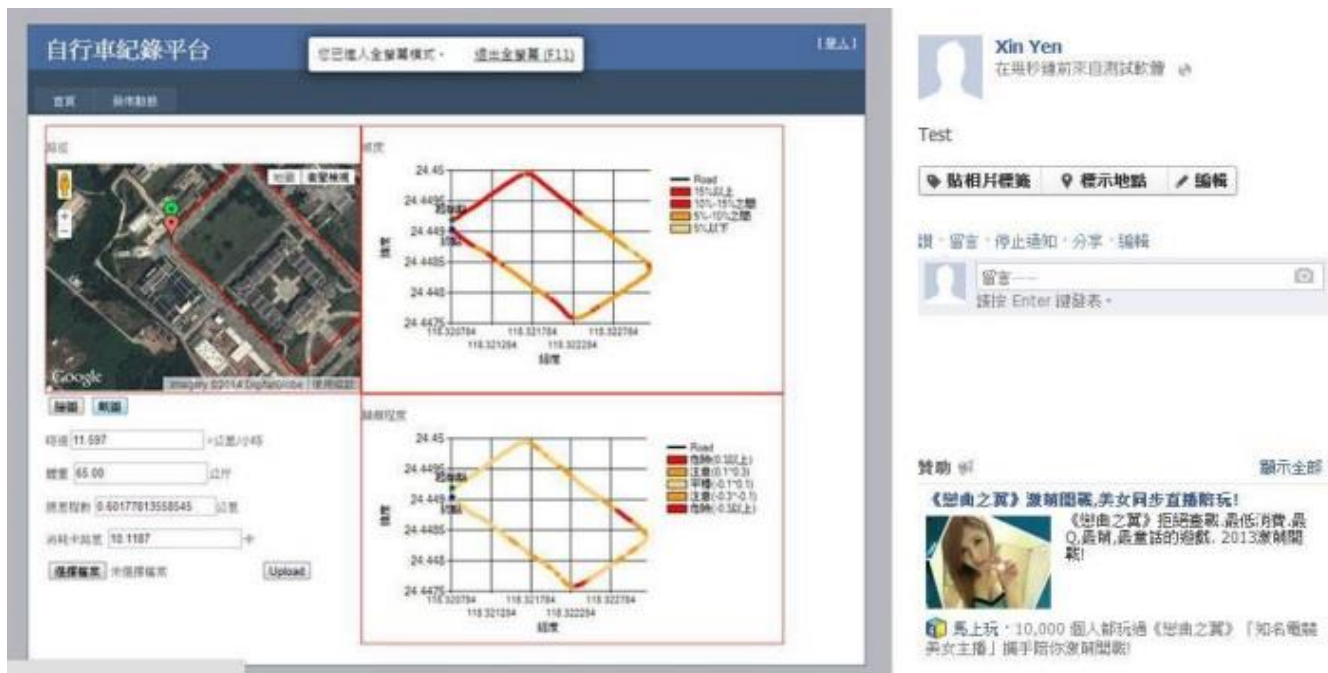| Cycling – Duration 1 hour	130 lb	155 lb	180 lb	205 lb
Cycling, mountain bike, bmx	502	598	695	791
Cycling, < 10 mph, leisure	236	281	327	372
Cycling, 10 - 11.9 mph, light	354	422	490	558
Cycling, 12 - 13.9 mph, moderate	472	563	654	745
Cycling, 16 - 19 mph, racing	708	844	981	1117
Stationary Cycling, light	325	387	449	512
Stationary Cycling, moderate	413	493	572	651
Stationary Cycling, vigorous	620	739	858	977

Fig. 22. Examples of information-sharing on a social networking website.

Riding Conditions

Riding conditions showed the balance state of the cyclists for the full duration of their cycling. Data recorded by the gyroscope module were calculated and converted to simple information, as shown in Figure 21.
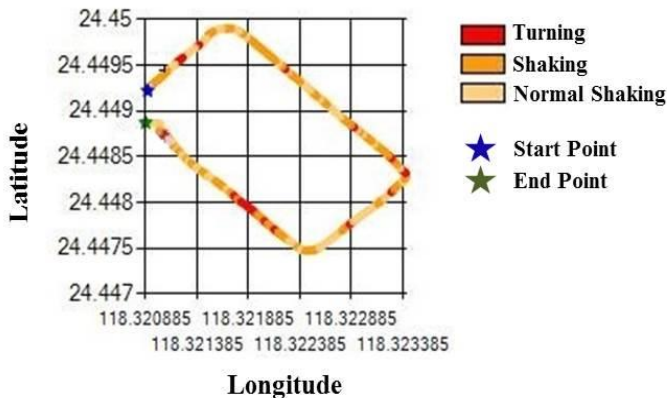

Fig. 21. Riding conditions.

C. Information Sharing

Screenshots of the results, displayed in the form of diagrams, were saved. A bicycle recording platform was used to collect this information and subsequently generate statistical results. The results were shared with other cycling enthusiasts on various social networking websites in the form of diagrams to convey information regarding the overall cycling environment. This allowed for the sharing of detailed cycling route information. Examples of this information-sharing are shown in Figure 22.

V. CONCLUSION

This study developed a smartphone-based real-time information feedback system for bicycles, providing cyclists with information while they are cycling. Smartphones were used for information display and calculation. To use the system introduced in this study, cyclists are only required to install the aforementioned modules and copy these programs to their smartphones. This system is expected to provide cyclists with a complete exercise-related information. Just as how a coach instructs professional cyclists, this system provides cyclists with information about the effectiveness of their exercise when cycling, helping cyclists to achieve their exercise goals. Also, the proposed system allows cyclists to share cycling information online. This information is useful for other cyclists who have not traveled along the route before. Overall, this study attempted to develop a bicycle record system of ground conditions based on IoT that can provide cyclists with accurate real-time information, thus enabling cyclists to enjoy a well-equipped cycling environment.

REFERENCES

[1]   X. Jinhua and G. Yun, "Research on humanization in bicycle design," *Computer-Aided Industrial Design and Conceptual Design (CAIDCD)*, pp. 1-5, Nov. 2006.

This article has been accepted for publication in a future issue of this journal, but has not been fully edited. Content may change prior to final publication. Citation information: DOI 10.1109/ACCESS.2017.2740419, IEEE Access

10

[2]   E. Fleisch, "What is the Internet of Things? - An Economic Perspective," *Auto-ID Labs White Pap*, WP-BIZAPP-053, 1-27, 2010.

[3]   F. Mattern, and C. Floerkemeier, "From the Internet of Computers to the Internet of Things," *Informatik-Spektrum*, 33 (2), 107-121, 2010.

[4]   C. Outram, C. Ratti, and A. Biderman, "The Copenhagen Wheel: An innovative electric bicycle system that harnesses the power of real-time information and crowd sourcing," *In Proceedings of the International Conference on Ecological Vehicles and Renewable Energies*, 2010.

[5]   K. Flüchter, F. Wortmann, and E. Fleisch, "Digital Commuting: The Effect of Social Normative Feedback on E-bike Commuting - Evidence from a Field Study," *In ECIS 2014 Proceedings*, 2014.

[6]   S. Eisenman, E. Miluzzo, N. Lane, R. Peterson, G. S. Ahn, and A. Campbell, "The BikeNet mobile sensing system for cyclist experience mapping," *SenSys'07*. pp. 87-101, 2007.

[7]   M. Y. Chiu, R. Depommier, and T. Spindler, "An Embedded Real-time Vision System for 24-hour Indoor/Outdoor Car-Counting Applications," *ICPR 3*, page 338-341, 2004.

[8]   K. Y. Lin, M. W. Hsu, and S. R. Liou, "Bicycle management systems in anti-theft, certification, and race by using RFID," *Cross Strait Four-Regional Radio Science and Wireless Technology Conference*, pp. 1054-1057, July 2011.

[9]   J. Y. Kim, C. G. Song, and N. G. Kim, "A new VR bike system for balance rehabilitation training," *7th Conf. Virtual Syst. Multimedia*, 2001.

[10]   K. Chen, Y. Zhang, and J. Yi, "Modeling rider/bicycle interactions with learned dynamics on constrained embedding manifolds," in *Proc. IEEE/ASME Int. Conf. Adv. Intell. Mechatronics*, Wollongong, Australia, pp. 442-447, 2013.

[11]   L. Zhang, J. Liu, H. Jiang, and Y. Guan, "SensTrack: Energy-efficient location tracking with smartphone sensors," *IEEE Sensors Journal*, 13 (10), pp. 3775-3784, 2013.

[12]   E. Thammasat and J. A. Chaicharn, "simply fall-detection algorithm using accelerometers on a smartphone," in *Proceedings of the Biomedical Engineering International Conference (BMEiCON)*, Ubon Ratchathani, Thailand, December 2012.

[13]   B.N. Ferreira, V. Guimaraes, and H. S. Ferreira, "Smartphone based fall prevention exercises," *2013 IEEE 15th International Conference on e-Health Networking, Applications & Services (Healthcom)*, pp. 643-647, Oct. 2013.

[14]   A. Anjum and M.U. Ilyas, "Activity recognition using smartphone sensors," *Consumer Communications and Networking Conference (CCNC)*, 2013 IEEE, pp. 914-919, Jan. 2013.

[15]   P. Buddharaju and N.S.C.P. Pamidi, "Mobile Exergames - Burn Calories While Playing Games on a Smartphone," *2013 IEEE Conference on Computer Vision and Pattern Recognition Workshops (CVPRW)*, pp. 50-51, June 2013.

[16]   Y. Shin and B.C. Wunsche, "A smartphone-based golf simulation exercise game for supporting arthritis patients," *2013 International Conference of Image and Vision Computing New Zealand (IVCNZ)*, pp. 459-464, Nov. 2013.

[17]   R. Van Der Merwe, "Sigma-point Kalman filters for probabilistic inference in dynamic state-space models," Ph.D. dissertation, Oregon Health Sci. Univ., Portland, OR, 2004.

[18]   J. Ambadan and Y. Tang, "Sigma-point Kalman filter data assimilation methods for strongly nonlinear systems," *J. Atmos. Sci.*, vol. 66, no. 2, pp. 261-285, Feb. 2009.

[19]   M. VanDyke, J. Schwartz, and C. Hall, Unscented Kalman Filtering for Spacecraft Attitude State and Parameter Estimation, Blacksburg, VA2004.

[20]   D. Simon, "Kalman Filtering," *Embedded Systems Programming*, vol. 14, no. June, pp. 72-79, 2001.

[21]   R. Faragher, "Understanding the Basis of the Kalman Filter Via a Simple and Intuitive Derivation," *IEEE Signal Process. Mag.*, vol. 29, no. September, pp. 128-132, 2012.